

The velocity peaks in the cold dark matter spectrum on Earth

P. Sikivie^{1,2}, I. I. Tkachev^{3,4} and Yun Wang³

¹Physics Department, University of Florida, Gainesville, FL 32611

²Institute for Theoretical Physics, Santa Barbara, CA 93106

³NA SA /Ferm ilab Astrophysics Center, FNAL, Batavia, IL 60510

⁴Institute for Nuclear Research, Russian Academy of Sciences, Moscow 117312, Russia

(April 13, 1995)

Abstract

The cold dark matter spectrum on earth is expected to have peaks in velocity space. We obtain estimates for the sizes and locations of these peaks. To this end we have generalized the secondary infall model of galactic halo formation to include angular momentum of the dark matter particles. This new model is still spherically symmetric and it has self-similar solutions. Our results are relevant to direct dark matter search experiments.

PACS numbers: 98.80.Cq, 95.35.+d, 14.80.Mz, 14.80.Ly

There is considerable evidence that galaxies are surrounded by dark halos which contribute 90% or more of the galactic mass [1]. Identifying the nature of the dark matter is the goal of considerable theoretical and experimental effort. The leading dark matter candidates are baryons, neutrinos, weakly interacting massive particles (WIMPs) and axions. From the point of view of galaxy formation, axions and WIMPs have identical properties which earn them the name of cold dark matter (CDM). Unlike baryonic dark matter, CDM is guaranteed to have negligible interactions other than through its gravitational effects. Unlike neutrinos, CDM has negligibly small primordial velocity dispersion. Studies of large scale structure formation support the view that the dominant fraction of dark matter is CDM. Moreover, if some fraction of the dark matter is CDM, it necessarily contributes to galactic halos by falling into the gravitational wells of galaxies. The main focus of our paper is to study the growth of galactic halos by the infall of cold dark matter, including the effect of angular momentum, and thence to derive properties of the spectrum of dark matter particles on Earth.

We are motivated in part by the prospect that a direct search experiment may some day measure that spectrum. In particular, if a signal is found in the cavity detector of galactic halo axions [2,3], it will be possible to measure the spectrum with great precision and resolution. Naturally, the question arises what can be learned about our galaxy from analyzing such a signal. Moreover, knowledge of the spectrum, which is identical for both CDM candidates, may help in the discovery of a signal.

In many past discussions of dark matter detection on earth, it has been assumed that the dark matter particles have an isothermal distribution. Thermalization has been argued to be the result of a period of "violent relaxation" [4] following the collapse of the protogalaxy. If it is strictly true that the velocity distribution of the dark matter particles is isothermal, which seems to be a very strong assumption, then the only information that can be gained from its observation is the corresponding virial velocity and our own velocity with respect to its standard of rest. If, on the other hand, the thermalization is incomplete, a signal in a dark matter detector may yield additional information.

J.R. Ipser and one of us discussed [5] the extent to which cold dark particles are thermalized in a galactic halo and concluded that there are substantial deviations from a thermal distribution in that the highest energy particles have narrow peaks in velocity space. There is one velocity peak on earth due to particles falling onto the galaxy for the first time, one peak due to particles falling out of the galaxy for the first time, one peak due to particles falling into the galaxy for the second time, and so on. A simple topological argument shows that these peaks exist no matter what is the distribution of angular momenta the dark matter particles have with respect to the galactic center, although angular momentum may reduce the sizes of the peaks. The peaks due to particles which have fallen in and out of the galaxy a large number of times in the past are washed out by scattering in the gravitational wells of stars, globular clusters and large molecular clouds. Those particles are in effect thermalized. But the peaks due to particles which have fallen in and out of the galaxy only a few times in the past are not washed out by scattering.

The width of the peaks due to the primordial velocity dispersion of the CDM particles is very small: $\Delta E = m \cdot 10^{-18}$ for axions and $\Delta E = m \cdot 10^{-14}$ for WIMPs, where m is the mass of the particles and ΔE their energy spread. As just mentioned, the peaks fragment because of the gravitational scattering of the particles by inhomogeneities in the galaxy. They also fragment because of structure formation on scales smaller than that of the galaxy as a whole. We expect that such structure formation in the CDM component of the matter density would be inhibited by the tidal forces of the galaxy's gravitational field, but some of it no doubt occurs. At any rate, it is clear that the peaks due to particles which have fallen in and out of the galaxy only a small number of times in the past are not entirely washed out by either scattering or small structure formation. It is the purpose of the present paper to estimate the sizes and locations of these peaks and we will no longer concern ourselves with their widths. Let us point out however that the sensitivity of the search for galactic halo axions using the cavity detector may be increased by looking for narrow peaks. Specifically, it is found that the signal to noise ratio of the upcoming axion search at LLNL [3] is increased by a factor $180f_1$ by looking for narrow peaks, where f_1 is the fraction of the local axion

density in the largest of the peaks of width $E < 10^{-11}$ m.

The tool we use to obtain estimates of the locations and sizes of the highest energy peaks is the secondary infall model of galactic halo formation [6]. In its original form, this model makes the following assumptions:

1) the dark matter is non-dissipative; 2) it has negligible initial velocity dispersion; 3) the gravitational potential of the galaxy is spherically symmetric and is dominated by the dark matter contribution; 4) the dark matter particles have zero angular momentum and therefore move on radial orbits through the galactic center.

Below, we will generalize the model to rid it of the fourth assumption. For clarity, we refer to the model with the fourth assumption included as the radial infall model.

An initial overdensity profile $M_i(r)$ is assumed. The equations of motion for the radial coordinate $r(\alpha; t)$ of each spherical shell (α is a shell label, t is time) in the gravitational potential due to all the other shells must then be solved for initial conditions given by the Hubble expansion at some arbitrarily chosen but early time t_i : $r(\alpha; t_i) = H(t_i)r(\alpha; t_i)$. Much progress in the analysis of the model came about as a result of the realization that the evolution of the galactic halo is self-similar [7] provided the initial overdensity has the following scale-free form:

$$\frac{M_i}{M_0} = \frac{M_0}{M_i} ; \quad (1)$$

where M_i and M_0 are respectively the mass and excess mass interior to r_i at the initial time t_i , i.e.

$$M_i(r_i) = \frac{4}{3} \bar{\rho}(t_i)r_i^3 + M_0(r_i); \quad (2)$$

where $\bar{\rho}(t_i) = 3H(t_i)^2/8\pi G = 1/6 G t_i^{-2}$ is the average density in a critical ($\Omega = 1$) universe, t_i having been chosen during the matter-dominated epoch. M_0 and α are constants characterizing the model. Self-similarity means that the phase-distribution of dark matter particles is time-independent after all distances have been rescaled by the overall size $R(t)$ of the galactic halo, all masses by the mass $M(t)$ interior to the radius $R(t)$, and all velocities

by $\sqrt[3]{GM(t)=R(t)}$. For the sake of definiteness, $R(t)$ is taken to be the "turn-around" radius at time t , i.e. the radius at which particles have zero radial velocity for the first time in their history (see Fig.1). In a self-similar solution, the motion of each shell is the same after the appropriate rescaling, i.e. $r(r;t) = r(r)(t=t(r))$, where $r(r)$ and $t(r)$ are respectively the turn-around radius and time of shell r . Also the mass profile of the halo is time-independent after rescaling, i.e. $M(r;t) = M(r)M(r=R(t))$. $r(r)$ and $M(r)$ are functions of a single variable which can be accurately obtained by numerical integration. In the limit $\beta \rightarrow 0$ it was shown analytically [7] that, $M(r)/r^3 \rightarrow 0$ if $\beta < 3$ and $M(r)/r^{3-(1+\beta)}$ if $\beta > 3$. The numerical integrations confirm this. Thus, for the range $0 < \beta < 3$, the radial infall model produces flat rotational curves, i.e. it is in accord with the main feature of the galactic mass distribution.

To fit the model to our present galactic halo we must determine appropriate values of $R(t_0)$ and $M(t_0)$, where t_0 is the age of the universe. First, we have:

$$t_0 = \frac{v_{\text{rot}}}{2} \sqrt{\frac{R(t_0)^3}{2GM(t_0)}} = \frac{6.52 \cdot 10^9 \text{ year}}{h}; \quad (3)$$

where h parametrizes the present Hubble rate: $H_0 = h \cdot 100 \text{ km sec}^{-1} \text{ Mpc}^{-1}$. The first equality in Eq.(3) follows from the fact that a given shell does not cross any other shell till after the moment of its first turnaround and therefore the mass interior to it stays constant till then. The second equality in Eq. (3) follows from the assumption $\beta = 1$ which is necessary to have a self-similar solution. Second, we match the rotation velocity in the model to the observed one for our galaxy:

$$v_{\text{rot}} = (r) \sqrt[3]{\frac{GM(t_0)}{R(t_0)}} = 220 \text{ km sec}^{-1}; \quad (4)$$

where (r) is extracted from the numerical solution of the model. Combining Eqs. (3) and (4), we have:

$$R(t_0) = \frac{1.32 \text{ Mpc}}{h(r)}; \quad (5)$$

For typical values of β and h , $R(t_0)$ turns out to be in the 1 to 3 Mpc range; see Table I. This is consistent with the value one would infer by taking nearby galaxies as tracers of mass.

Indeed M 31, at a distance of 0.73 M pc, is falling towards us with a line-of-sight velocity of 120 km /s, whereas galaxies at distances exceeding 3 M pc are receding from us as part of the universal Hubble expansion. In fact, turning this around, Eqs. (4) and (5) could form a basis for estimating the age of the universe.

Figs.1 and 2 show the phase-space diagram and the velocity peaks on earth for $\beta = 0.2$ and $h = 0.7$. Our distance to the galactic center is taken to be $r_s = 8.5$ kpc. The rows labeled $j = 0:0$ in Table I give the density fractions and kinetic energies of the first five incoming peaks in the radial infall model. For each incoming peak there is an outgoing peak with approximately the same energy and density fraction (see Fig 2). Note that, because of the scale invariance of the model, increasing h at fixed β is equivalent to decreasing $R(t_0)$ keeping the observation radius r_s fixed, or to increasing r_s at fixed $R(t_0)$. We find that, in the radial infall model, the sizes of the two peaks due to particles falling in and out of the galaxy for the first time are large, each containing of order 10% of the local halo density for in the standard CDM model inspired [8] range of 0.1 – 0.3.

However, because the radial infall model neglects the angular momentum that the dark matter particles are expected to have, we must question its reliability in this context. In particular, since in that model all particles go through the galactic center at each pass, the halo density is large there, behaving as $\rho_{\text{halo}}(r) \propto \frac{1}{r^2 \ln(1+r)}$. Instead, the actual halo mass distribution has the approximate form $\rho_{\text{halo}}(r) = \rho_{\text{halo}}(0) / (1 + (r/a)^2)$, where a , called the core radius, is of order a few kpc [9]. Since r_s and a have the same order of magnitude, the corrections due to angular momentum are not small. Moreover, angular momentum affects most the peaks with the highest energies (the ones we are most interested in) because these are the ones due to particles which have come from furthest away.

Fortunately, there is a generalization of the radial infall model which takes angular momentum into account while still keeping the model tractable. In this generalization, each shell is divided into N subshells labelled by an index k , ($k = 1, \dots, N$). The particles in a given subshell ($;k$) all have the same magnitude $l_k(r)$ of angular momentum. At each point on each subshell, the distribution of angular momentum vectors is isotropic about the

axis from that point to the galactic center. Thus the spherical symmetry of each subshell is maintained in time. Moreover, the evolution is self-similar provided:

$$l_k(t) = j_k r(t)^2 = t(t); \quad (6)$$

where the j_k are a set of dimensionless numbers characterizing the galaxy's angular momentum distribution. In Eq.(6) we are neglecting the small dependence of the turn-around radius $r(t)$ and time $t(t)$ upon k , although that neglect is not necessary for self-similarity. The model will be described in detail elsewhere [10]. Let us just give here the two equations:

$$\frac{d^2 r_k}{dt^2} = -\frac{j_k^2}{8 r_k^3} M(t) \frac{r_k(t)}{r(t)^2}; \quad (7a)$$

$$M(t) = \frac{2}{3} \sum_{k=1}^N n_k \frac{d}{r(t)^{1+2/3}} \frac{r_k(t)}{r(t)^2}; \quad (7b)$$

and the boundary conditions: $r_k(1) = 1$, $\dot{r}_k(1) = 0$, which determine the model's evolution through $r_k(t) = r(t) r_k(t/t)$ and $M(r,t) = M(t) M(r/R(t))$. In Eq. (7a), n_k is the mass fraction contributed by the subshell k . In all cases presented here, the j_k are taken to be distributed according to the density

$$\frac{dn}{dj} = \frac{2j}{j_0^2} \exp(-j^2/j_0^2); \quad (8)$$

We report our results in terms of the average $j = \sqrt{\sum_{j=0}^{\infty} j^2} = j_0 = 2$. Fig.3 shows the rotation curves for the case $\alpha = 0.2$, $j = 0$ (whose phase-space diagram and velocity peaks are shown in Figs.1 and 2) and the case $\alpha = 0.2$, $j = 0.2$. It shows that the effect of angular momentum is to give a core radius to the galactic halo distribution. The definition of core radius we use below to report our results is the radius b at which half of the rotation velocity squared is due to the halo. For the density profile $\rho(r) = \rho(0)/(1 + (r/a)^2)$, $b = 2.33a$; of course, our density profiles are only qualitatively similar to that one. Fig. 4 shows the velocity peaks for the case $\alpha = 0.2$, $j = 0.2$, $h = 0.7$. Table I gives the values of the current turn-around radius $R(t_0)$, the core radius b , the halo density at our location $\rho(r_s)$, and the density fractions

and energies of the j most energetic incoming peaks for various values of α , j and h . The range of α values chosen is motivated by models of large-scale structure formation [8] as well as by the flatness of the rotation curves produced. Table I is the summary of our results.

In conclusion, we have generalized the radial infall model of galactic halo formation to include the effect of angular momentum, all the while keeping the model spherically symmetric and self-similar in its time evolution. The galactic halo distributions we obtain have core radii as well as flat rotation curves. We find that the contribution to the local halo density due to particles which are falling in and out of the galaxy for the first time or which have passed through the galaxy only a small number of times in the past, and which are therefore not thermalized, is rather large, comprising several percent per velocity peak. Finally let us emphasize that the peak sizes we obtain are only order of magnitude estimates since they are averages over a broad distribution of possible angular momenta.

ACKNOWLEDGMENTS

We thank S. Colombi, J. Ipser, J. Primack and D. Spergel for useful discussions. This research was supported in part by the DOE and NASA grant NAGW-2381 at Fermilab, and the DOE grant DE-FG 05-86ER 40272 at the University of Florida.

REFERENCES

- [1] For reviews, see e.g., V. Trimble, *Ann. Rev. Astron. Astrophys.* 25 (1987) 425; E. W. Kolb and M. S. Turner, *The Early Universe*, Addison-Wesley, 1988; M. Srednicki, Editor *Particle Physics and Cosmology: Dark Matter*, North-Holland, 1990.
- [2] P. Sikivie, *Phys. Rev. Lett.* 51 (1983) 1415 and *Phys. Rev. D* 32 (1985) 2988; L. Krauss, J. Moody, F. Wilczek and D. Morris, *Phys. Rev. Lett.* 55 (1985) 1797; S. D'Elia et al., *Phys. Rev. Lett.* 59 (1987) 839 and *Phys. Rev. D* 40 (1989) 3151; C. Hagmann et al., *Phys. Rev. D* 42 (1990) 1297.
- [3] K. van Bibber et al., "Status of the Large-Scale Dark-Matter Axion Search", LLNL preprint UCRL-JC-118357, to be published in the Proceedings of the International Conference on Critique of the Sources of the Dark Matter in the Universe, Berkeley, CA, February 16-18, 1994.
- [4] D. Lynden-Bell, *MNRAS* 136 (1967) 101.
- [5] J. R. Ipser and P. Sikivie, *Phys. Lett. B* 291 (1992) 288.
- [6] J. E. Gunn and J. R. Gott, *Ap. J.* 176 (1972) 1; J. R. Gott, *Ap. J.* 201 (1975) 296; J. E. Gunn, *Ap. J.* 218 (1977) 592; C. Pryor and M. Lecar, *Ap. J.* 269 (1983) 513.
- [7] J. A. Fillmore and P. Goldreich, *Ap. J.* 281 (1984) 1; E. Bertschinger, *Ap. J. Suppl.* 58 (1985) 39.
- [8] Y. Hoffman and J. Shaham, *Ap. J.* 297 (1985) 16; P. J. Quinn, J. K. Salmon and W. H. Zurek, *Nature* 322, 329 (1986); M. M. Crone, A. E. Evrard and D. O. Richstone, *Ap. J.* 434, 402 (1994).
- [9] J. Bahcall, *Astrophys. J.* 287 (1984) 926; M. S. Turner, *Phys. Rev. D* 33 (1986) 889.
- [10] P. Sikivie, I. I. Tkachev and Yun Wang, in preparation.

TABLES

TABLE I. Relative magnitudes A_k and kinetic energies E_k of the first five incoming peaks for various values of β , j and h . Also shown are the current turn-around radius R in units of Mpc , the core radius b in kpc , and the local density ρ in $10^{-25} \text{ g cm}^{-3}$. The A_k are in percent and the E_k are in units of $0.5 (300 \text{ km s}^{-1})^2$.

	j	h	R	b	ρ	$A_1 (E_1)$	$A_2 (E_2)$	$A_3 (E_3)$	$A_4 (E_4)$	$A_5 (E_5)$
0.2	0.0	0.7	2.0	0.0	8.1	13 (4.0)	5.3 (3.2)	3.3 (2.7)	2.4 (2.4)	1.9 (2.2)
1.0	0.0	0.7	0.9	0.0	8.4	1.6 (3.4)	1.1 (3.2)	0.9 (3.0)	0.8 (2.9)	0.7 (2.8)
0.15	0.2	0.7	2.4	13	5.0	4.0 (3.1)	5.4 (2.3)	5.3 (1.8)	4.9 (1.5)	4.0 (1.3)
0.2	0.1	0.7	2.0	4.5	7.6	7.4 (3.8)	7.2 (3.0)	4.9 (2.5)	3.2 (2.2)	2.4 (2.0)
"	0.2	0.7	2.0	12	5.4	3.1 (3.4)	4.1 (2.6)	4.3 (2.1)	4.1 (1.8)	3.6 (1.6)
"	"	0.5	2.8	17	4.9	1.9 (3.5)	2.5 (2.7)	2.8 (2.3)	2.9 (2.0)	3.0 (1.7)
"	"	0.9	1.6	9.3	6.0	4.4 (3.2)	5.3 (2.5)	5.1 (2.0)	4.5 (1.7)	3.6 (1.5)
"	0.4	0.7	2.0	40	2.6	0.8 (2.5)	1.6 (1.8)	2.1 (1.4)	2.4 (1.1)	2.6 (0.9)
0.25	0.2	0.7	1.8	8.5	5.5	2.0 (3.5)	2.9 (2.8)	3.3 (2.4)	3.4 (2.1)	3.1 (1.8)
0.4	0.2	0.7	1.5	2.2	7.7	1.1 (4.0)	1.5 (3.4)	1.8 (3.0)	1.9 (2.8)	2.1 (2.5)

FIGURES

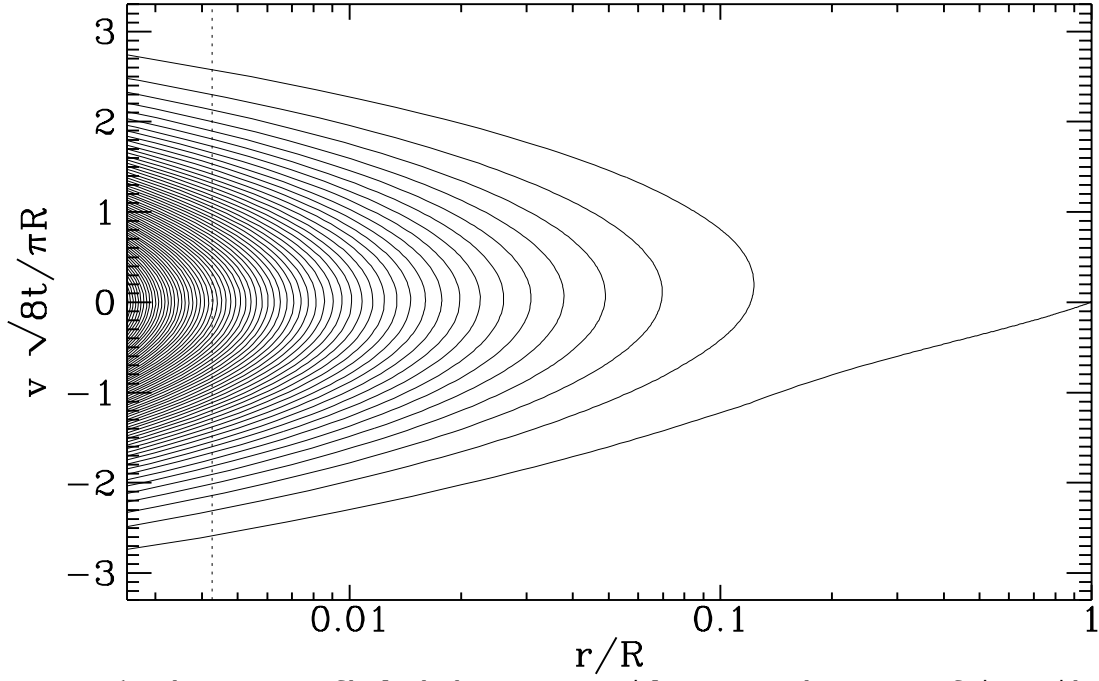


FIG .1. Phase space of halo dark matter particles at a fixed moment of time with $\alpha = 0.2$ and $j = 0$. Dotted line corresponds to the Sun's position if $h = 0.7$.

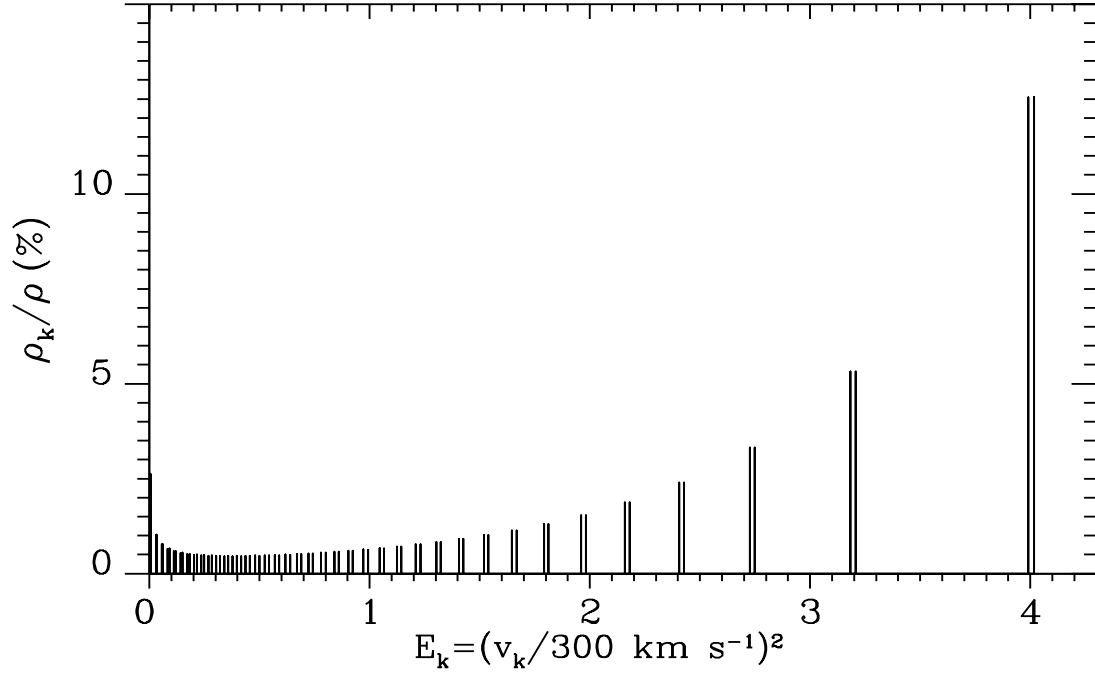


FIG .2. The spectrum of velocity peaks at the Sun's position for the case $\alpha = 0.2$, $j = 0$ and $h = 0.7$.

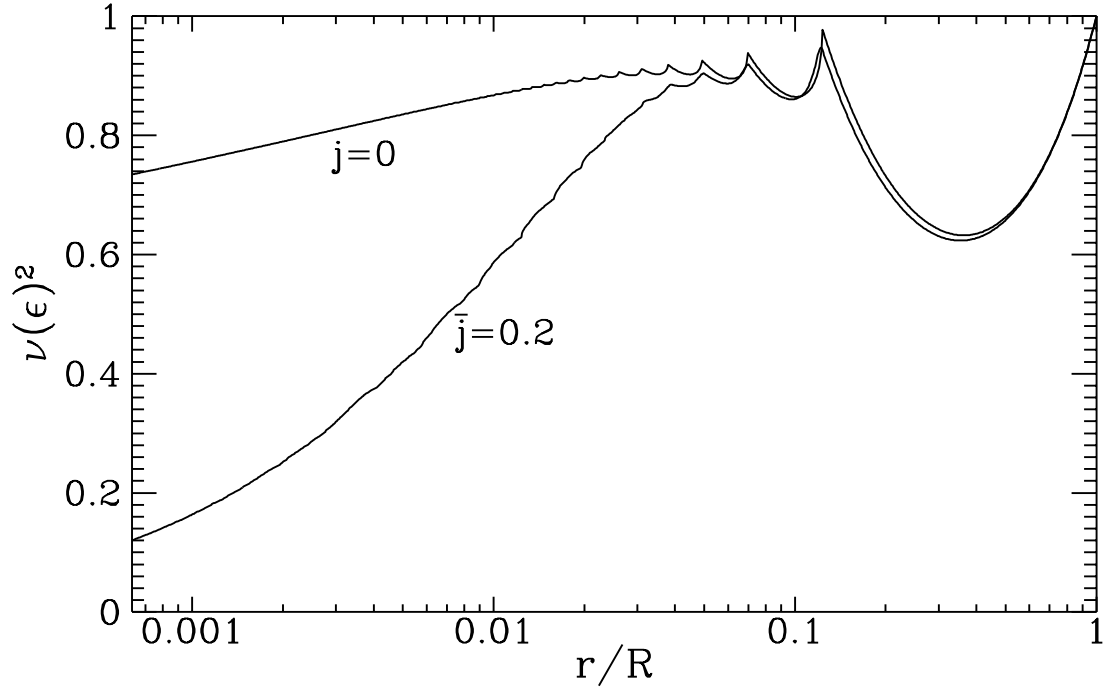


FIG .3. Rotational curves for the case $\alpha = 0.2$, with and without angular momentum .

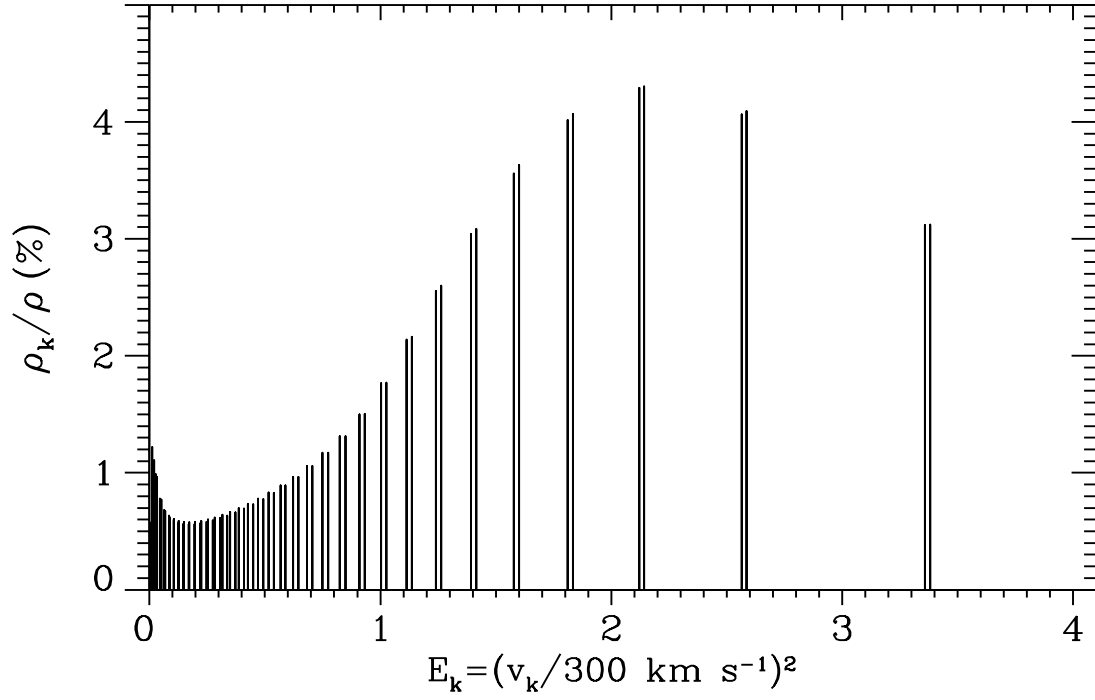


FIG .4. The spectrum of velocity peaks for the case $\alpha = 0.2$, $j = 0.2$ and $h = 0.7$.